USING A THERMAL IMAGER TO QUANTIFY BURIED THERMAL STRUCTURE IN NATURAL SNOW

Cora Shea[1], Bruce Jamieson[1*] and Karl Birkeland[2]

[1] Department of Civil Engineering, Department of Geoscience, University of Calgary, Canada
[2] USDA Forest Service National Avalanche Center, Bozeman, Montana, USA

ABSTRACT: Avalanche researchers and practitioners have long measured snowpack temperatures in snow pits with thermometers about 10 cm apart. This led to the assumptions that temperature gradients are smooth and that temperature changes are regular. For this study, we used a thermal imager in standard snow pits in the Canadian Rocky Mountains during two seasons between 2010 and 2012. We collected the first season of data in a very shallow, below treeline snowpack study plot, and the second season of data in a deeper, treeline study plot. Data included thousands of thermal images, as well as visual macro images of the snow crystals in each pit layer to monitor changes.

We observed strong temperature gradients on the scale of individual snow crystals. We found that these small scale gradients correlated with future snow crystal changes. We also found that these gradients changed quickly with the weather, even at depth. This paper focuses on our most recent findings from the 2011-12 season, and describes our overall progress in extracting data from thermal images to use for research and forecasting. We use correlations to present very general relationships between thermal data, crystal size, and layer stability tests. We also present temperature and gradient changes at depth during a period of clearing.

1. INTRODUCTION

On the ground, the seasonal snowpack changes over time. With its complex ice connections and air-filled pore spaces, the dry snowpack constantly builds and rebuilds its structure from within. The movement of water vapour is a key mechanism in the metamorphism of dry snow. Water vapour—the brick and mortar of future snow structure—leaves warm crystal surfaces and travels to deposit on colder ones, changing the shape and size of crystals (Kaempfer and Plapp, 2009).

Historically, snow pit temperatures have played almost no role in forecasting of dry snow avalanches. Although studies have found that colder snow is stiffer and therefore stronger (e.g. Schweizer, 1996), when examining differences between stable and unstable dry snowpacks, temperature was not a strong indicator (Schweizer and Wiesinger, 2001). Yet objective assessments of crystal change and consequent snow stability are much desired by forecasting programs.

So the interest in temperatures continues. Seo et al. (2008) correlated typical 10 cm spaced temperatures to crystal size, but they found that the data set of pits needed was extensive and the relation only held for a small area and one season. Rather than use temperatures to develop a highly specific model, we envision thermal imaging being used – at least for the present time – to detect physical processes and trends that are not apparent using traditional methods. Thermal imaging of the pit wall may be of greater interest to those interested in temperature gradients within the snowpack, e.g. avalanche practitioners, than those interested in absolute temperatures, e,g. snow hydrologists.

Hence, our overall motivation as researchers was to help develop easy-to-use field methods for obtaining thermal data. We outline a few such methods here. This paper presents a selection of our observations, and some tactics to extract data from thermal images.

2. METHODS

We used two different cameras. In the 2010-11 season, a FLIR B300 was used, with a 0.05°C between-pixel sensitivity, a resolution of 240x320 pixels, and a 25° viewing angle. In the 2011-12 season, a FLIR P660 was used, with a 0.03°C between-pixel sensitivity, a resolution of and 480x640 pixels, and a 18° x 24° viewing angle. For all daily visits at both study sites, images and measurements were made between approximately noon and 14:00 local time.

* *Corresponding author address*: Bruce Jamieson, Department of Civil Engineering, 2500 University Drive NW, Calgary, Alberta, Canada T2N 1N4; tel: 1-403-220-7479; email: bruce.jamieson@ucalgary.ca

Thermal imaging the pit wall is subject to errors not encountered with thermometers inserted into the pit wall. Once exposed, the new surface (skin) of a pit wall adjusts towards an energy balance with the atmosphere, and is subject to operator heating (Shea and Jamieson, 2010). A temperature change of a degree within a minute is plausible. Two of the faster effects are incoming shortwave and outgoing long wave. The effect of incoming shortwave is minimized by using a shaded pit wall and quickly imaging the pit wall. The effect of outgoing longwave is reduced by quickly imaging the pit wall, and would be further reduced by a cloudy sky. Also, heat from the snowpack could preferentially flow along more conductive layers like crusts towards the pit wall, potentially increasing local gradients. However, Shea et al. (2012) showed that the gradients smoothed within the first few minutes, suggesting equilibration with the environment dominated any differential lateral heat flow along the layers.

We used one study site during the 2010-11 season and another during the 2011-12 season. Both sites were nearly flat with minor rolls inclined at less than 5°, and with open skyview. The main geographical characteristics of each site are noted in Table 1. Our motivation for the 2010-11 season was to determine if the thermal camera could see anything useful on a snowpit wall. To this end, we chose a very shallow snowpack to maximize the temperature gradients and crystal growth. A graphical overview of the season, with all pits on the daily visits, and a selection of pits from the hourly visits on 3 March 2011 is shown in Figure 1.

2.1 Tests, layers, and crystal images

We used the compression test (CT) to assess layer stability in the 2011-12 season. One observer performed all CT tests, recording both taps and fracture character (Greene et al., 2010). Taps were used directly in the correlations in Section 3.2, with 35 taps indicating no result. Fracture character was rated on a 0-5 scale, where 0 = No Result, 1 = Break, 2 = Progressive Compression, 3 = Resistant Planar, 4 = Sudden Collapse, and 5 = Sudden Planar. While this order is plausible for an increase in propagation potential, it lacks supporting data.

Macro crystal images were obtained on every visit using a Nikon P5100 camera with a macro setting and a magnifier attached to the lens. Crystals were placed on a 3 mm grid for size reference, and cooled while being photographed by placing the crystal screen on snow. At least four images were obtained of crystals from each layer of interest (described below), as well as the layers in-between when the snowpack was shallow.

To minimize error in the identification of crystal size and type:

- All of the crystal images for the season were assessed at the same time after the winter, to minimize any change in observer error from day to day.
- The days were assessed out of order to reduce observer bias toward trends over time, and to remove other contextual information such as stability test results.
- The average minimum and maximum crystal size for each layer were assessed separately, and the midpoint of these extremes was used as the average crystal size.

As the snowpack gained depth and layers during the 2011-12 season, there was no longer enough time to track every layer using thermal and macro crystal images on each visit. Hence, four layers were tracked:

1. Depth hoar, formed prior to the start of observations, and first observed 26 November 2011.
2. Surface hoar, formed between 3 and 10 December 2011, and first observed 10 December 2011.
3. Near surface facets, formed between 10 and 17 December 2011, and first observed 17 December 2011.
4. Surface hoar, formed between 28 January and 4 February 2012, and first observed 4 February 2012.

No CT test results occurred while each layer was still on the surface, although crystal size and gradients were available on those visits; hence, the difference in sample size in Table 2. Also, the depth hoar was not observed on the surface.

Two of the four layers (the depth hoar, and the December surface hoar layers) “reactivated” during the observation period. That is, they fractured in CT tests, and then had no result for one or more weeks, and then fractured subsequently in CT tests.

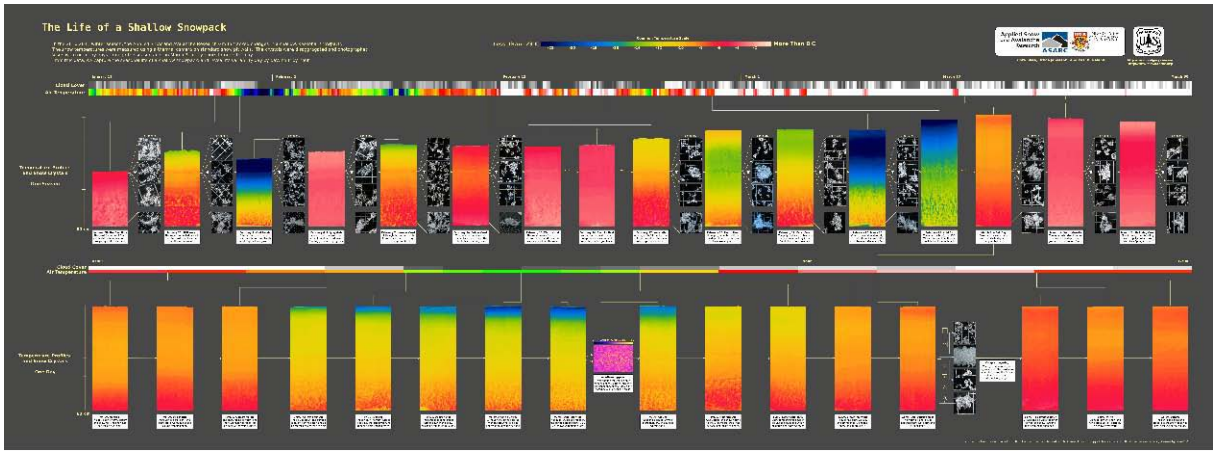

Figure 1: A small preview of the full-size overview image from the 2010-11 study plot. The full version is available online at http://webapps2.ucalgary.ca/~asarc/files/ShallowSnowPoster Shea Jan2012.png

Table 1: Differences between the 2010-11 study and the 2011-12 study. In addition to the visits over the course of each season, we performed an hour-by-hour change study between 02:00 and 22:00 local time on 3 March 2011, and between 05:00 and 11:00 local time on 24 March 2012.

		Location		Site visits		
Season	Snow depth	Coordinates	Elevation	Dates	Number	Frequency
2010-11	35-66 cm	51.045◦ N, -115.417◦ W	1650 m (BTL)	28 Jan - 30 Mar	17	every 2-4 days
2011-12	70-205 cm	50.802◦ N, -115.289◦ W	2150 m (TL)	26 Nov -17 Mar	18	weekly

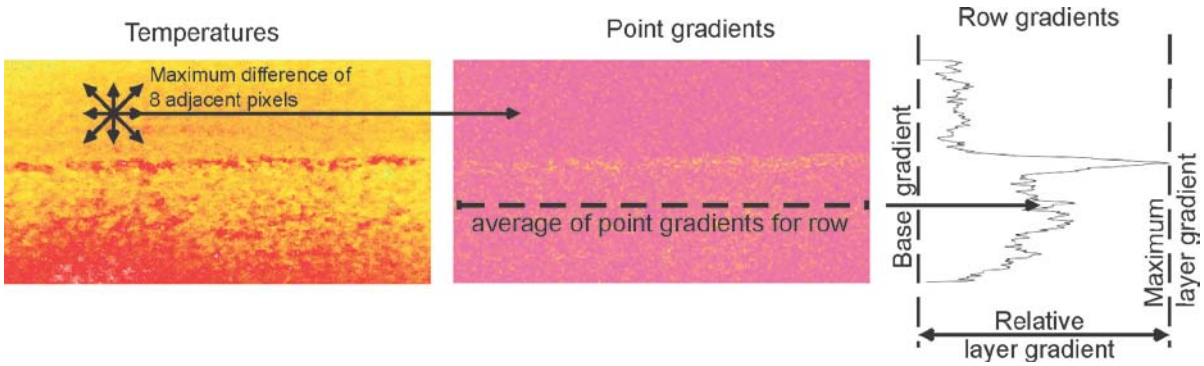

Figure 2: Methods used for obtaining gradients for the layers described in Section 2.1 and whose correlations with other observations are presented in Table 2. In the temperature image (left), a point gradient is calculated as the maximum difference between the point temperature and the eight adjacent pixel temperatures. By averaging the point gradients from each row in the gradient array (middle image), we obtained row gradients in the right graph. The base and maximum gradients are the minimum and maximum gradients for the layer including the adjacent snow in the manual snow profile (right graph).

2.2 Thermal image data

For the 2011-12 season data, we selected a few variables that could be obtained from the thermal images. For the long-term correlations discussed in Section 3.2, we used *maximum layer gradients* and *relative layer gradients*, the calculations of which are shown in Figure 2. A more precise discussion of gradients and their relation to the distance over which they were measured can be found in Shea et al. (2012).

For the hourly study on 24 March 2012, the point gradient values were averaged to create one gradient value for each area.

2.3 Field controls on thermal imagery

All of the corrections and techniques discussed in Shea et al. (2012) were applied in both winters, excluding the lens corrections. Thus, for both seasons:

- The snow pit walls were shaded
- The initial pit on each daily visit was dug back deeper than the snowpack depth
- The pit wall was photographed within 90-120 seconds of exposure
- Each area of interest was imaged multiple times, for gradient comparisons
- Areas of interest were centered to minimize lens effects
- Emissivity was set to E = 0.98
- Air temperature was recorded

In the 2010-11 season, the lens was characterized using the same small area of the pit wall in different parts of different images (0.004°C difference per degree of lens angle, on average. Shea et al., 2012).

For 2011-12, we wished to develop an alternative set of corrections which were faster and easier. When using the more sensitive camera, it became apparent that the linearity of the lens corrections may have been due to the lesser sensitivity of the B300. With the P660, the angle effect on snow images were quite obviously a cosine relationship (Figure 3), which matches theory (Wolfe and Zissis, 1978).

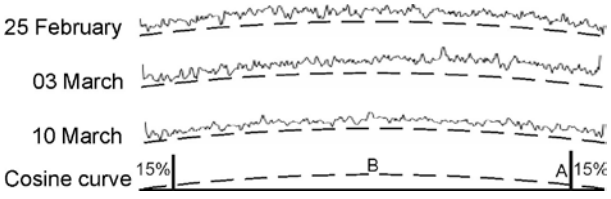

Figure 3: Comparison of row gradients to ideal cosine curves between ±9° lateral view (upper three graphs). Cropping the cosine curve by 15% laterally at A results in a 35% reduction in curve height at B.

Cutting off at least the outer 15% of pixels on each edge results in an overall lens effect across the image lower than the 0.03°C camera sensitivity. Specifically, cutting the view on each side from 9° (half of 18°) to 7.7° reduces the magnitude of change in a cosine curve by about 35%. In the case of snow gradient effects, this reduced the row gradients from slightly above equipment sensitivity (0.036°C at the maximum image extent) to less than equipment sensitivity (0.022°C at the cropped image extent).

This new, rougher form of "correction" is a compromise. To focus on an area of concern, such as a weak layer, and using only a few images, the pixel-by-pixel corrections from the earlier paper are the best way to ensure the image field has been corrected for average snow roughness effects. But a typical visit to a deep snowpack would produce upwards of 30 images. Correcting every pixel in these images requires (a) enough past data to properly characterize the lens for the snowpack, and (b) significant computer processor time. Cropping, on the other hand, takes minutes and requires only knowledge of the lens angle, i.e. no past data are needed.

Other effects, such as equalization of the sensor, constant hand angle while taking photos, and consistent time after pit exposure between shots, - make comparison more difficult. Some tips are included in the earlier paper. Additional simple field methods can be developed, such as counting out loud when clearing the wall, and ensuring that images of the same area occur at similar times after exposing the wall.

3. RESULTS AND DISCUSSION

3.1 Communication

We distributed a poster overview of the 2010-11 results (Figure 1) to various forecasting offices. It was enthusiastically received. The poster does not present new observations or methods, but rather provides a visual reference of extreme temperature swings and crystal size changes over a season.

Based on this positive reception, thermal data, gradient data, and crystal images from this study were released nearly every week to the public online during the 2011-12 season. Our study site is located in a popular recreation area, and we shared the web address of the data with most visitors who came over to inquire and observe the study in progress each Saturday. This process was also received positively. We recommend such open sharing of research data in the future, along

with a disclaimer against using it for decision making.

3.2 Correlations between snowpack variables during 2011-12

3.2.1 Gradient correlations

The temperature gradients of the selected layers correlated with crystal size, CT taps and CT fracture character. The strong gradient correlation with future crystal size makes physical sense, as gradients persisting into the afternoon hours—when these observations were made—could be strong enough to change crystal sizes one week out. This is discussed further in Section 3.3. Shorter time steps would be of interest for future work.

Our result that gradients correlate with CT results in the past and future suggest that this site was dominated by prolonged periods of stability and instability of the tracked layers. Further, these prolonged periods correlated with the increased and decreased temperature gradients. Comparable lead times have been previously observed, e.g. the average age of a weak layer for unstable human-triggered avalanches in a combined Canada-Switzerland study was around 11 days. Further, although activity usually ranged on layers with ages 6 to 14 days, avalanches were observed up to 56 days later (Schweizer and Jamieson, 2001).

3.2.2 Crystal size versus CT results

Average crystal size had no correlation to present or past CT results (Table 2). Indeed most studies use difference in crystal size between an anticipated weak layer and the layers above and below, or the crystal *type*, as a method of snow profile interpretation (McCammon and Schweizer, 2002; Schweizer and Jamieson, 2007). Hence, these correlations are only shown for comparison.

We are unsure why crystal size correlated with future CT results but not current CT results. Possible explanations include:

- Crystal size was our only subjective measurement, and this may be a form of observer bias. Although crystals were assessed from multiple photographs, and out of order for the days observed, this is worth mentioning and is very difficult to assess and control.
- The correlation may be random chance. The correlation between CT fracture character and crystal size is not significant, and the significance on CT taps is $p = 0.04$, implying a one in 25 chance of the correlation occurring in random data.
- The correlation may be due to a weather event that skewed the data set. With a small data set, it is possible to leverage a weak correlation which would not hold in general. The most extreme values supporting this correlation came from a period of very warm weather (likely a cohesive slab that transmitted the dynamic stresses to the weak layer) following a period of very cold weather (likely crystal growth in the weak layer).
- The correlation may have physical basis in that larger crystals are more likely to continue to grow, and be more susceptible to critical loading by snowfall or CT taps.

In the studies relating snow profile properties to skier triggering, the mean difference between crystal size sets were quite small, less than 1 mm, for crystals 1-2 mm in extent. Here, the difference in means between days with CT results (fractures with ≤ 30 taps) and days with no CT results on each layer is similar (0.5 mm) but non-significant. This non-significance, however, is perhaps due to the small sample size as well, or the small difference in means when compared to the mean crystal extent overall (around 5 mm).

Regardless, this finding serves as a strong reminder that further work is needed.

3.2.3 Depth versus CT results

These correlations were included for comparison with findings from other studies. They match the physical knowledge that as damping snow overlying a specific weak layer increases, the number of taps needed also increases. The fracture character trend was for less frequent sudden fractures for deeper layers.

The lack of temporal correlation in the past or future could be because of the two layers which "reactivated", as described in Section 2.

3.3 By day

In the spring of 2011, we observed rapid changes in gradients with weather changes. This was observed both at our 2010-11 study plot in the hourly study on 3 March, and in a research trip to Silverton, Colorado in an unplanned series of observations. One of the case studies in Shea et al. (2012) describes the hourly study on 3 March, and attributes the temperature changes around a persistent crust to be due to latent heat flux.

These observations intrigued us, and motivated us to see if they would also occur in a deeper snowpack in the winter of 2011-12. Figure 4 shows

Table 2: Selected correlations between snowpack variables with values from the previous week, current visit and following week. Correlations with $p \leq 0.01$ are **bold**, with $0.05 \geq p > 0.01$ are underlined, all other are non-significant. For the gradient and crystal size comparisons in the first two rows, n = 49. For the other comparisons, n = 46 for reasons described in Section 2.1. For future and past comparisons, the sample size is reduced by 8, as each data set is offset by one at the beginning and one at the end, for each of the four layers included. For an explanation of the types of gradients, see Figure 2.

Snowpack variables		Correlations between current observation and snowpack variable 2 at different visits			Section
Variable 1 (current obs.)	Variable 2	Past week	Current visit	Future week	
Max. gradient	Avg. crystal size	**0.47**	**0.47**	**0.72**	3.2.1
Max. gradient	Crystal size change (week prior)	0.07	0.16	0.36	3.2.1
Relative gradient	CT taps	**-0.43**	**-0.47**	**-0.40**	3.2.1
Relative gradient	CT fracture char.	**0.40**	**0.52**	**0.39**	3.2.1
Avg. crystal size	CT taps	-0.11	-0.01	-0.32	3.2.2
Avg. crystal size	CT fracture char.	0.12	0.03	0.28	3.2.2
Depth of layer	CT taps	0.32	**0.43**	0.24	3.2.3
Depth of layer	CT fracture char.	-0.29	**-0.40**	-0.30	3.3.3

our findings from an hourly study on the morning of 24 March 2012. It was cloudy and snowing prior to the first pit being dug.

The average gradient within a small area of the snow pit, even at depths of 1 m or more, appears to increase when the air temperature cooled and the sky cleared, thereby increasing longwave radiation losses from the snow surface. This remarkable finding is consistent with our measurements from 2010-11 (Figure 1; Shea et al., 2012). For some reason a cooling snow surface appears to quickly affect temperature gradients at layer boundaries on the pit wall deep in the snowpack.

The gradients apparently moderate shortly after the first direct sun hit the snow surface. This helps explain why the correlations in Section 3.2 are as strong as they are despite an entire week elapsing between each of the past, present, and future values. As described in Section 2, observations were taken at or shortly after noon for the day visits. So, if and when a gradient persisted into midday, it was arguably intermittently strong enough to cause significant change in snow structure over long time periods such as a week.

One limitation of our work is that after exposing the first pit we were only able to dig back around 70 to 100 cm for each subsequent pit wall due to time constraints. We think that the effect of differential heat flow along the more conductive layers is small based on Shea et al. (2012) who found temperature gradients only smoothed slightly in the first few minutes after the pit wall was exposed. We also infer that the effect of the short exposure time on gradients is small because the changes in the gradients in the depth hoar—with less sky view—mimic the changes in the upper layers.

4. CONCLUDING REMARKS

We presented correlations between thermal gradients, stability tests, and crystal size for four layers—surface hoar, near-surface facets, and depth hoar—over the course of a season. Though we cannot offer physical explanations for all of the significant correlations, we believe our results make a compelling baseline for future work. Also, our data set is small and only from one area.

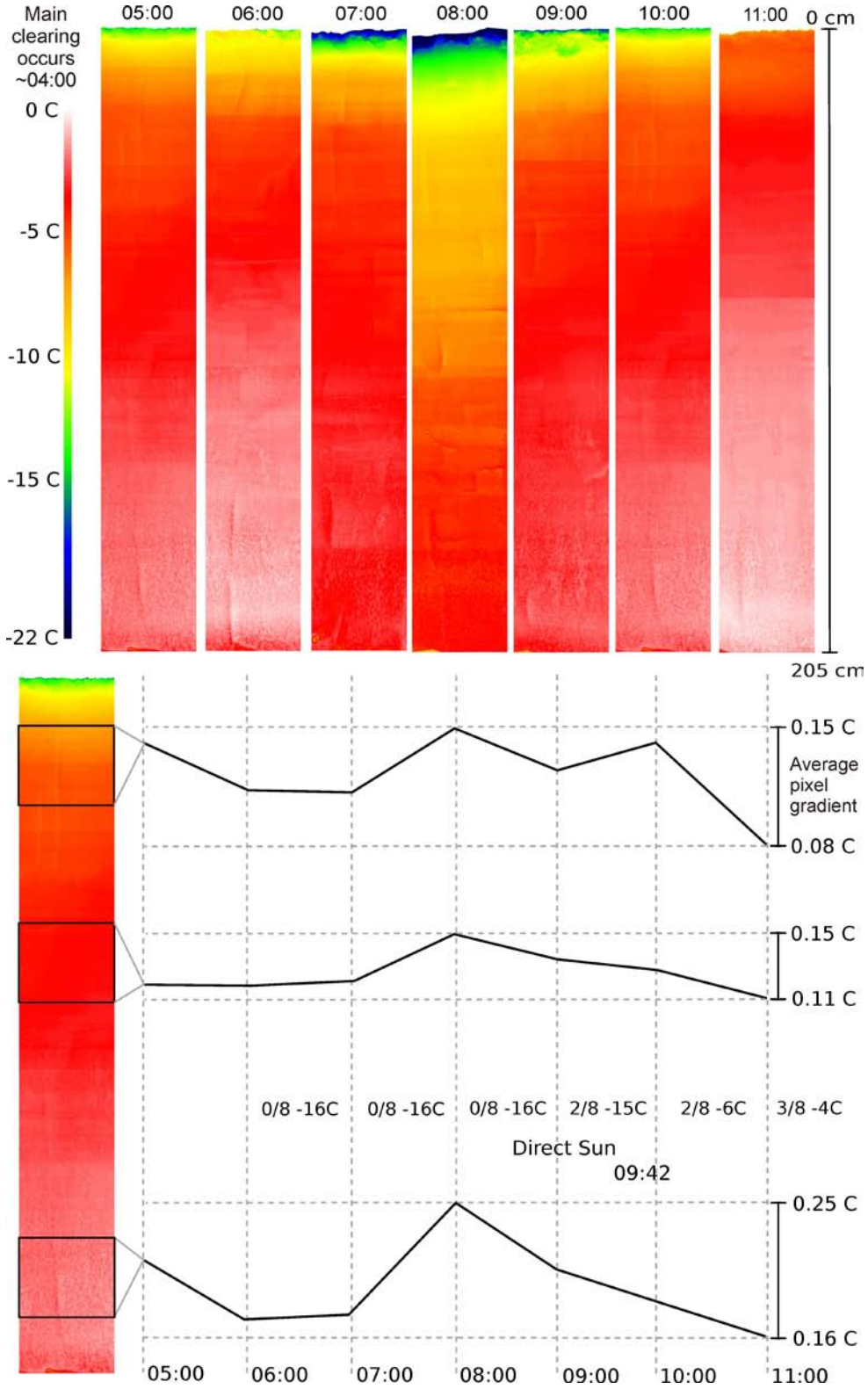

Figure 4: Graphical summary of findings from the hourly study on 24 March 2012. The depth hoar consistently showed higher gradients both here and on our daily visits. Average point gradients for 0.08 and 0.25°C per pixel, when scaled to 10 cm distance, are equivalent to 11 to 35°C per 10 cm. The horizontal shade change in the composite image for 11:00 am is at the boundary between images; such temperature jumps occur occasionally when combining images.

We also presented changes observed over the course of hours in a relatively deep snowpack during a period of sky clearing and surface cooling. The speed and depth of thermal activity due to weather events is an unprecedented and as yet unexplained observation, as it occurs faster than snow conducts heat. It is possible that a rapid change in temperature near the snow surface drives a local change in vapour pressure that might then "propagate" down through the snowpack, increasing vapour movement. Differences in latent heat exchange along layer boundaries might then increase temperature gradients along those boundaries.

These possibilities can be investigated in future field studies and possibly with cellular automata models. We hope this work inspires others to answer the many questions that remain.

Thermal imaging remains a promising technology for research, education, and—perhaps in the future—forecasting. Previously, we could not observe and measure small-scale temperatures and gradients, and we could not quantify many interesting thermal conditions that might drive metamorphic changes in the snowpack. Further study is needed to see whether our observations translate elsewhere, especially to different seasons and snow climates.

5. ACKNOWLEDGEMENTS

We are grateful to TECTERRA for access to the FLIR 660 during the 2011-12 season, and to Jon Neufeld of TECTERRA for many enthusiastic and engaging conversations on use of thermal imaging of snow. For financial support, the Canadian authors thank the Natural Sciences and Engineering Research Council of Canada, HeliCat Canada, the Canadian Avalanche Association, Mike Wiegele Helicopter Skiing, Teck Mining Company, Canada West Ski Areas Association, the Association of Canadian Mountain Guides, Backcountry Lodges of British Columbia, and the Canadian Ski Guides Association. Thanks to Ryan Buhler, Sascha Bellaire and Scott Thumlert for proofreading.

REFERENCES

Greene, E., Birkeland, K., Elder, K., Landry, C., Lazar, B., McCammon, I., Moore, M., Sharaf, D., Sterbenz, C., Tremper, B., Williams, K., 2010, Snow, Weather, and Avalanches: Observational Guidelines for Avalanche Programs in the United States: American Avalanche Association, Pagosa Springs CO, 150 pp.

Kaempfer, T. and Plapp, M., 2009. Phase-field modeling of dry snow metamorphism. *Physical Review*, 793:031502, 1–17.

McCammon, I. and Schweizer, J., 2002. A field method for identifying structural weaknesses in the snowpack. Proceedings of the International Snow Science Workshop, Pentiction, *British Columbia, 30 September to 4 October 2002*, 471-488.

Schweizer, J., 1996. Preliminary results on controlled shear experiments. Proceedings of the 1996 International Snow Science Workshop, 195–197.

Schweizer, J. and Jamieson, B., 2001. Snow cover properties for skier triggering of avalanches. *Cold Regions Science and Technology*, 33: 207–221.

Schweizer, J. and Jamieson, B., 2007. A threshold sum approach to stability evaluation of manual snow profiles. *Cold Regions Science and Technology*, 47: 50–59.

Schweizer, J. and Wiesinger, T., 2001. Snow profile interpretation for stability evaluation. *Cold Regions Science and Technology*, 33: 179–188.

Seo, D., Azar, A., Khanbilvardi, R., and Powell, A., 2008. Analysis of snowpack properties and estimation of snow grain size using clpx data. *Geoscience and Remote Sensing Symposium, IEEE International*, 4: 1034–1037.

Shea, C. and Jamieson, B., 2010. Some fundamentals of handheld snow surface thermography. The Cryosphere 5, 55-66. Online at http://www.the-cryosphere.net/5/55/2011/

Shea, C., Jamieson, B., and Birkeland, K., 2012. Use of a thermal imager for snow pit temperatures. *The Cryosphere*, 6: 287–299. Online at www.the-cryosphere.net/6/287/2012/.

Wolfe, W.L. and Zissis, G.J., 1978. *The Infrared Handbook*. The Infrared Information and Analysis Center IRIA Center, Environmental Research Institute of Michigan. Prepared for The Office of Naval Research, Department of the Navy, Washington, DC and Arlington, VA.